ProbStat Forum, Volume 11, April 2018, Pages 19–35
ISSN 0974-3235

ProbStat Forum is an e-journal.
For details please visit www.probstat.org.in

The Poisson Weibull-X family of distributions

Mansoor M[a], Tahir M H[b], Gauss Cordeiro[c], Ayman Alzaatreh[d], Zuabir M[e]

[a]*Department of Statistics, Govt Degree College Liaqatpur, Pakistan.*
[b]*Department of Statistics, The Islamia University of Bahawalpur, Pakistan.*
[c]*Department of Statistics, Federal University of Pernambuco, Recife-50740-540, PE, Brazil.*
[d]*Department of Mathematics and Statistics, American University of Sharjah, Sharjah, UAE.*
[e]*Department of Statistics, Govt. S.E College, Bahawalpur, Pakistan.*

Abstract. A new compound family of lifetime distributions is introduced to deal with lifetime data. We study some of its structural properties. A special model of the family, called the Poisson Weibull-Pareto (PWP) model, is defined. Its density can have shapes such as left-skewed, approximately symmetric and right-skewed. It can also accommodate different hazard shapes such as reversed-J, increasing, decreasing and upside-down bathtub. Various properties of this model are investigated including shape properties, quantile function, explicit expressions for the ordinary and incomplete moments and generating function. The ability of maximum likelihood approach to estimate parameters is assessed by a simulation study. Three real life data sets have been analyzed, and the PWP model provides adequate fits.

1. Introduction

The Weibull distribution is a well-known distribution named after the Swedish physicist Weibull (1951) who studied its application to fly ash and strength of material in 1951. It was further studied by Kao (1956) who applied it to the failure of electronic components and systems, and since then, it has been extensively used for analyzing lifetime data. The Weibull model has also been used for modeling phenomenon with monotone failure rates. When modeling monotone hazard rates, the Weibull distribution may be an initial choice because of its negatively and positively skewed density shapes. However, it does not provide reasonable parametric fits for modeling phenomenon with non-monotone failure rates such as the bathtub shaped and the unimodal failure rates. In the last few years, new classes of extended Weibull distributions have been defined to provide more flexible failure rates. A review of some of these models includes the exponentiated-Weibull by Mudholkar and Srivastava (1993), beta-Weibull by Famoye et al. (2005) and Kumaraswamy-Weibull by Cordeiro et al. (2010), among others. However, most of the generalizations were motivated from mathematical interests.

Recently, Alzaatreh et al. (2013) defined the cumulative distribution function (cdf) of the *Weibull-X* family by

$$H(x;\boldsymbol{\xi}) = 1 - \exp\left(-\left\{-\log\left[1 - G(x)\right]\right\}^{c}\right). \tag{1}$$

2010 *Mathematics Subject Classification*. 60E05, 62E15, 62N05.
Keywords. Compounding, Pareto distribution, Weibull-X family, Weibull distribution, zero-truncated Poisson distribution.
Received: 31 October 2017; Revised: 24 February 2018, Accepted: 09 March 2018

Email addresses: mansoor.abbasi143@gmail.com (Mansoor M), mtahir.stat@gmail.com (Tahir M H), gausscordeiro@gmail.com (Gauss Cordeiro), aalzaatreh@aus.edu (Ayman Alzaatreh), zubair.stat@yahoo.com (Zuabir M)

The probability distribution function (pdf) corresponding to (1) is given by

$$h\left(x;\boldsymbol{\xi}\right)=\frac{c\,g(x)}{1-G(x)}\,\left\{-\log\left[1-G(x)\right]\right\}^{c-1}\,\exp\left(-\left\{-\log\left[1-G(x)\right]\right\}^{c}\right). \tag{2}$$

The main objective of this paper is to propose a new family of lifetime distributions with a strong physical motivation. As explained below, it can give better fits than many known lifetime models, which is an interesting property. The paper is unfolded as follows. In Section 2, we define the new family and study some of its special members. In Sections 3 and 4, we obtain a linear representation for the density and derive some general properties. In Section 5, we study some mathematical properties of PWP model. In Section 6, the model parameters are estimated by the method of maximum likelihood. In Section 7, we explore the flexibility of the PWP model by means of three applications to real data. Finally, Section 8 offers some concluding remarks.

2. The new compound family

In this section, we give a physical motivation for the new family. Consider that a system has N subsystems functioning independently at a given time, where N is a truncated Poisson random variable with probability mass function

$$\mathbb{P}(N=n)=\frac{\lambda^{n}}{n!(\mathrm{e}^{\lambda}-1)},\quad n=1,2,\ldots.$$

Suppose that the failure time of each subsystem has the *Weibull-X* distribution defined by the cdf given in Equation (1) (for $x>0$). Further, let Y_i denote the failure time of the ith subsystem and X denote the time to failure of the first out of N functioning subsystems. We can write $X=\min\left(Y_1,\ldots,Y_N\right)$. The conditional cdf of X given N is

$$F(x\mid N)\;=\;1-\mathbb{P}\big(X>x\mid N\big)=1-\left[\mathbb{P}(Y_1>x)\right]^{N}=1-\mathbb{P}\left[1-H\left(x;\boldsymbol{\xi}\right)\right]^{N}.$$

Thus, the unconditional cdf of X (for $x>0$) can be expressed as

$$\begin{aligned}F(x)\;&=\;1-\frac{1}{\mathrm{e}^{\lambda}-1}\sum_{n=1}^{\infty}\frac{\left\{\lambda\left[1-H\left(x;\boldsymbol{\xi}\right)\right]\right\}^{n}}{n!}\\&=\;\frac{1-\exp\left[-\lambda\,H\left(x;\boldsymbol{\xi}\right)\right]}{1-\mathrm{e}^{-\lambda}}\end{aligned}$$

and then

$$F(x;\lambda,c,\boldsymbol{\xi})=\frac{1-\exp\left(-\lambda[1-\mathrm{e}^{-\{-\log[1-G(x)]\}^{c}}]\right)}{1-\mathrm{e}^{-\lambda}}. \tag{3}$$

Further, we can omit sometimes the dependence on the vector $\boldsymbol{\xi}$ of the baseline parameters λ and c and write $F(x)=F(x;\lambda\,c,\boldsymbol{\xi})$ and also $f(x)=f(x;\lambda,c,\boldsymbol{\xi})$. The pdf corresponding to Equation (3) reduces to

$$\begin{aligned}f(x)\;&=\;\frac{\lambda\,c\,g(x)\,\left\{-\log\left[1-G(x)\right]\right\}^{c-1}\,\mathrm{e}^{-\{-\log[1-G(x)]\}^{c}}}{(1-\mathrm{e}^{-\lambda})\left[1-G(x)\right]}\\&\times\;\exp\left(-\lambda\left\{1-\mathrm{e}^{-\{-\log[1-G(x)]\}^{c}}\right\}\right),\end{aligned} \tag{4}$$

where $g(x)$ is the baseline pdf. Equation (4) will be most tractable when $G(x)$ and $g(x)$ have simple analytic expressions. In the rest of this section and in Sections 3 and 4, a random variable X with cdf (3) is denoted by $X\sim\mathrm{PWX}(\lambda,c,\boldsymbol{\xi})$.

Remark 2.1. *The cdf and pdf in Equations* (3) *and* (4) *can be expressed in terms of the hazard and cumulative hazard functions of $g(x)$ as follow*

$$F(x) = \frac{1 - \exp\left(-\lambda[1 - \mathrm{e}^{-(H_g(x))^c}]\right)}{1 - \mathrm{e}^{-\lambda}}$$

and

$$f(x) = \frac{\lambda\, c}{1 - \mathrm{e}^{-\lambda}}\, h_g(x)\, (H_g(x))^{c-1} \mathrm{e}^{-(H_g(x))^c} \exp\left(-\lambda[1 - \mathrm{e}^{-(H_g(x))^c}]\right),$$

respectively, where $h_g(x) = g(x)/[1 - G(x)]$ and $H_g(x) = -\log[1 - G(x)]$ are the hazard and cumulative hazard rate functions corresponding to the pdf $g(x)$.

The survival function (sf) and hazard rate function (hrf) of X are given by

$$S(x) = \frac{\exp\left(-\lambda[1 - \mathrm{e}^{(H_g(x))^c}]\right) - \mathrm{e}^{-\lambda}}{1 - \mathrm{e}^{-\lambda}},$$

and

$$h(x) = \frac{\lambda\, c\, h_g(x)\, (H_g(x))^{c-1} \mathrm{e}^{-(H_g(x))^c}}{1 - \exp\left(-\lambda[-\mathrm{e}^{-(H_g(x))^c}]\right)},$$

respectively.

Remark 2.2. *(i) The quantile function (qf) of the PWX family can be obtained by inverting Equation* (3) *as*

$$Q(u) = G^{-1}\left(1 - \exp\left[-\left\{ - \log[1 + \lambda^{-1} \log(1 - (1 - \mathrm{e}^{-\lambda})u)]\right\}^{1/c}\right]\right). \tag{5}$$

If U has a uniform $(0, 1)$ distribution, then the solution of the nonlinear equation $X = Q(U)$ has the density function given in Equation (4).
(ii) If T follows the compound Poisson uniform distribution, then

$$X = G^{-1}\left(1 - \mathrm{e}^{-\{-\log(1-T)\}^c}\right)$$

has the PWX family.
(iii) The shapes of the density and hrf of the PWX family are given by

$$\frac{g'(x)}{g(x)} + \frac{h_g(x)}{H_g(x)}\left[H_g(x) - c\,(H_g(x))^{c-1}\left(\lambda\,\mathrm{e}^{-(H_g(x))^c} + 1\right) + c - 1\right] = 0$$

and

$$\frac{g'(x)}{g(x)} + \frac{h_g(x)}{H_g(x)}\left[H_g(x) + c\,(H_g(x))^{c-1}\left(\frac{\lambda\,\mathrm{e}^{-(H_g(x))^c}}{\exp\left(\lambda \mathrm{e}^{-(H_g(x))^c}\right) - 1} - 1\right) + c - 1\right] = 0,$$

respectively, where $g'(x) = \frac{d}{dx}\, g(x)$.

2.1. Special PWX distributions

The PWX family (3) allows for greater flexibility of its tails and can be widely applied in many areas of engineering and biology. In this section, we present some of its special cases because it extends several widely-known distributions in the literature. In order to reduce redundancy in the scale parameters we set $\lambda = 1$ in all the members of PWX family.

2.2. The PW-Pareto (PWP) distribution

For the Pareto random variable with cdf $G(x) = 1 - \left(x/\theta\right)^{-\alpha}$ (for $x > \theta$), equation (3) reduces to

$$F(x) = \frac{1 - \exp\left(\mathrm{e}^{-\left[\alpha \, \log(x/\theta)\right]^c} - 1\right)}{1 - \mathrm{e}^{-1}}. \tag{6}$$

2.3. The PW-exponentiated-exponential (PWEE) distribution

If X follows the two-parameter exponentiated-exponential distribution with cdf $G(x) = \left(1 - \mathrm{e}^{-\theta x}\right)^{\alpha}$. The cdf of three-parameter PWEE distribution (for $x > 0$) is defined from (3) as

$$F(x) = \frac{1 - \exp\left(\mathrm{e}^{-\left\{-\log\left[1-\left(1-\mathrm{e}^{-\theta x}\right)^{\alpha}\right]\right\}^c} - 1\right)}{1 - \mathrm{e}^{-1}}$$

2.4. The PW-Lindley (PWL) distribution

Taking $G(x)$ to be the Lindley cumulative distribution with parameter $\theta > 0$, $G(x) = 1 - \left(\frac{1+\theta+\theta\,x}{1+\theta}\right) \mathrm{e}^{-\theta x}$, it follows the three-parameter PWL cdf (for $x > 0$)

$$F(x) = \frac{1 - \exp\left(\mathrm{e}^{-\left\{\theta x - \log\left[\frac{1+\theta+\theta x}{1+\theta}\right]\right\}^c} - 1\right)}{1 - \mathrm{e}^{-1}}$$

2.5. The PW-loglogistic (PWLL) distribution

The cdf of the LL distribution is (for $x, a, b > 0$) $G(x) = 1 - [1 + (x/a)^b]^{-1}$. Inserting this expression in (3) gives the PWLL cdf

$$F(x) = \frac{1 - \exp\left(\mathrm{e}^{-\left\{\log\left[1+(x/a)^b\right]^{-1}\right\}^c} - 1\right)}{1 - \mathrm{e}^{-1}}$$

2.6. The PW-Gumbel (PWGu) distribution

Consider the Gumbel distribution with location parameter $\mu \in \mathbb{R}$ and scale parameter $\sigma > 0$ and cdf (for $x \in \mathbb{R}$) given by $G(x) = \exp\left[-\exp\left(\frac{x-\mu}{\sigma}\right)\right]$. The mean and variance are equal to $\mu - \gamma\sigma$ and $\pi^2\sigma^2/6$, respectively, where γ is the Euler's constant ($\gamma \approx 0.57722$). Then, the PWGu cdf (for $x \in \mathbb{R}$) becomes

$$F(x) = \frac{1 - \exp\left(\mathrm{e}^{-\left\{-\log\left[1-\exp\left(-\exp\left(\frac{x-\mu}{\sigma}\right)\right)\right]\right\}^c} - 1\right)}{1 - \mathrm{e}^{-1}}$$

3. Linear representation of the density

In this section, we use three important results. First, for any real parameter c and $z \in (0, 1)$, the formula holds

$$[-\log(1 - z)]^c = z^c + \sum_{i=0}^{\infty} p_i(c)\, z^{i+c+1}, \tag{7}$$

where $p_0(c) = c/2$, $p_1(c) = c\,(3c+5)/24$, $p_2(c) = c\,(c^2+5c+6)/48$, $p_3(c) = c\,(15c^3+150c^2+485c+502)/5760$, etc, are Stirling polynomials.

Second, the exponential partial Bell polynomials in formal double series expansion are defined by

$$\exp\left(t \sum_{m\geq 1} z_m \frac{p^m}{m!}\right) = \sum_{n,k\geq 0} \frac{B_{n,k}}{n!}\, p^n\, t^k, \tag{8}$$

where

$$B_{n,k} = B_{n,k}(z_1, z_2, \ldots, z_{n-k+1}) = \sum \frac{n!}{c_1!\, c_2! \ldots (1!)^{c_1} (2!)^{c_2} \ldots} z_1^{c_1}\, z_2^{c_2}, \ldots,$$

and the summation is taken over all integers $c_1, c_2, c_3, \ldots \geq 0$ such that $c_1 + 2c_2 + 3c_3 + \cdots = n$ and $c_1 + c_2 + c_3 + \cdots = k$. The exponential partial Bell polynomials can be computed in *Mathematica* and *Maple* using BellY[n,k,{$z_1, \ldots, z_{n-k+1}$}] and IncompleteBellB(n, k, z[1], z[2],. . . , z[n-k+1]).

Third, we consider the *exponentiated-G* (exp-G) family with power parameter $\gamma > 0$ whose cdf and pdf are given by $\Pi(x) = G(x)^\gamma$ and $\pi(x) = \gamma\, G(x)^{\gamma-1}\, g(x)$, respectively. This method for generating exp-G distributions has received a great deal of attention in the last two decades and more than thirty exp-G models have already been published.

Expanding the exponential term and using the binomial expansion in Equation (3), we obtain

$$F(x) = \sum_{i=1}^{\infty} \left[a_{i,0} + \sum_{j=1}^{i} a_{i,j}\, \mathrm{e}^{-j\{-\log[1-G(x)]\}^c} \right], \tag{9}$$

where

$$a_{i,j} = \frac{(-1)^{i+j+1}\, \lambda^i}{i!(1-\mathrm{e}^{-\lambda})} \binom{i}{j}.$$

For $j \geq 1$, we can write from Equation (7)

$$\exp[-j\,\{-\log[1-G(x)]\}^c] = \exp[-j\, G(x)^c]\, \exp\big[-j\, G(x)^c \sum_{m=1}^{\infty} q_m\, G(x)^m\big],$$

where $q_m = q_m(c) = p_{m+1}(c)$ for $m \geq 1$. By expanding both exponentials, the second one using Equation (8), we obtain

$$\exp[-j\, G(x)^c] = \sum_{r=0}^{\infty} \frac{(-j)^r\, G(x)^{rc}}{r!}$$

and

$$\exp\big[-j\, G(x)^c \sum_{m=1}^{\infty} q_m\, G(x)^m\big] = \sum_{n,k\geq 0} \frac{(-j)^k\, B^{\star}_{n,k}}{n!}\, G(x)^{n+kc},$$

where $B^{\star}_{n,k} = B_{n,k}(q_1, 2!q_2, \ldots, (n-k+1)!q_{n-k+1})$.

Multiplying the last two expressions gives (for $j \geq 1$)

$$\exp[-j\,\{-\log[1-G(x)]\}^c] = \sum_{n,k,r\geq 0}^{\infty} \frac{(-j)^{k+r}\, B^{*}_{n,k}}{n!\, r!}\, G(x)^{n+(k+r)c}.$$

By inserting this result in Equation (9), we have

$$F(x) = K + \sum_{n,k,r\geq 0}^{\infty} t_{n,k,r}\, \Pi_{n,(k+r)c}(x), \tag{10}$$

where $\Pi_{n,(k+r)c}(x) = G(x)^{n+(k+r)c}$ is the cdf of the exp-G distribution with power parameter $n+(k+r)c > 0$, $K = \sum_{i=1}^{\infty} a_{i,0}$, $d_{k,r} = (-j)^{k+r} \sum_{i=1}^{\infty} \sum_{j=1}^{i} a_{i,j}$ and

$$t_{n,k,r} = \frac{d_{k,r}\, B^{\star}_{n,k}}{n!\, r!}.$$

We define the set $J = \{n, k, r \geq 0; n + (k + r)c > 0\}$. By differentiating Equation (9), we obtain

$$f(x) = \sum_{n,k,r \in J}^{\infty} t_{n,k,r}\, \pi_{n,(k+r)c}(x), \tag{11}$$

where $\pi_{n,(k+r)c}(x) = [n + (k + r)c]\, G(x)^{n+(k+r)c-1}\, g(x)$ is the exp-G density with power parameter $n + (k + r)c > 0$. Equation (11) reveals that the density of the PWX family is a linear mixture of exp-G densities. So, several of the family properties can be determined by knowing those properties of the exp-G model.

4. Some mathematical properties

In this section, we obtain the ordinary and incomplete moments, mean deviations and moment generating function (mgf) of X. General formulae for other quantities are not included for brevity but they are available from the authors upon request. Established algebraic expansions for some mathematical quantities of the PWX family can be more efficient than computing them directly by numerical integration of its density function. Analytical facilities available in programming softwares like `Mathematica`, `Maple`, `Matlab`, `Ox` and `R` can be used to apply these results in practice. Henceforth, let Z_a be a random variable having the exp-G(a) density with power parameter $a > 0$.

4.1. Moments

First, we derive the sth ordinary moment of X, say $\mu'_s = E(X^s)$. We have from Equation (11)

$$\mu'_s = \sum_{n,k,r \in J}^{\infty} t_{n,k,r}\, \mathbb{E}(Z^s_{n+(k+r)c}). \tag{12}$$

We provide a simple application of Equation (12) for the Poisson Weibull-Lomax distribution, where here Z_a refers to the exp-Lomax(a) distribution with shape parameters a and σ and scale parameter δ. The moments of Z_a are given by

$$\mathbb{E}(Z^s_a) = \gamma\, \delta^{-s} \sum_{p=0}^{s} \binom{s}{p} (-1)^p\, B\left(1 - \frac{s-p}{\sigma}, \gamma\right),$$

where $B(a, b) = \Gamma(a)\, \Gamma(b)/\Gamma(a + b)$ denotes the beta function.

Inserting this expression in Equation (12) gives

$$\mu'_s = \delta^{-s} \sum_{n,k,r \in J}^{\infty} \sum_{p=0}^{s} (-1)^p\, [n + (k + r)c]\, t_{n,k,r} \binom{s}{p} B\Big(1 - \frac{s-p}{\sigma}, [n + (k + r)c]\Big). \tag{13}$$

The nth central moment of X, say μ_n, is given by

$$\mu_s = \mathbb{E}(X - \mu'_1)^s = \sum_{n=0}^{s} \binom{s}{n} (-\mu'_1)^{s-n}\, \mu'_n,$$

where μ'_n is obtained from Equation (13).

The cumulants (κ_s) of X are determined recursively from

$$\kappa_s = \mu'_s - \sum_{n=0}^{s-1} \binom{s-1}{n-1} \kappa_n\, \mu'_{s-n},$$

where $\kappa_1 = \mu'_1$, $\kappa_2 = \mu'_2 - \mu'^2_1$, $\kappa_3 = \mu'_3 - 3\mu'_2\mu'_1 + \mu'^3_1$, etc. The skewness (γ_1) and kurtosis (γ_2) of X follow from the ordinary moments using well-known relationships.

The sth incomplete moment, say $\varphi_s(z)$, of X can be expressed from (11) as

$$\varphi_s(z) = \int_0^t x^s f(x)dx = \sum_{n,k,r\in J}^{\infty} t_{n,k,r} \int_0^z x^s \pi_{n,(k+r)c}(x)dx. \tag{14}$$

The last integral can be determined for most exp-G models. Let $M = Median(X) = Q(0.5)$ be the median of X. The amount of scatter in a population is evidently measured to some extent by the totality of deviations from the mean and median given by $\delta_1 = \mathbb{E}(|X - \mu_1'|)$ and $\delta_2 = \mathbb{E}(|X - M|)$, respectively. They can be expressed in term of the first incomplete moment as $\delta_1 = 2\mu_1' F(\mu_1') - 2\varphi_1(\mu_1')$ and $\delta_2 = \mu_1' - 2\varphi_1(M)$, respectively, where $F(\mu_1')$ comes from (3) and $\varphi_1(\cdot)$ is the first incomplete moment given by (14) with $s = 1$.

Another application of the first incomplete moment is related to the Bonferroni and Lorenz curves defined (for a given probability p) by $L(p) = \varphi_1(x_p)/\mu_1'$ and $B(p) = \varphi_1(x_p)/(p\mu_1')$, respectively, where x_p can be evaluated numerically by (5). These curves are very useful in economics, demography, insurance, engineering and medicine.

4.2. Generating function

We provide two explicit expressions for the mgf of X, say $M(t)$. First, we can write from Equation (11)

$$M(t) = \sum_{n,k,r\in J}^{\infty} t_{n,k,r}\, M_{n+(k+r)c}(t), \tag{15}$$

where $M_{n+(k+r)c}(t)$ is the mgf of $Z_{n+(k+r)c}$. Hence, the PWX generating function can be determined from the exp-G generating function (see Nadarajah and Kotz (2006)).

Secondly, the mgf of X can be expressed from Equation (11) as

$$M(t) = \sum_{n,k,r\in J}^{\infty} t_{n,k,r}\, (n + (k + r)c)\, \rho\big(t, n + (k + r)c\big), \tag{16}$$

where

$$\rho(t, a) = \int_{-\infty}^{\infty} \mathrm{e}^{\mathrm{t\,x}}\, \mathrm{G(x)^a\, f(x)dx} = \int_0^1 \exp\{\mathrm{t\, Q_G(u)}\}\, \mathrm{u^a du}.$$

5. Properties of the PWP distribution

In this section, we provide some structural properties of the PWP distribution. Most of these properties follow from the results in Section 4.

The pdf corresponding to (6) is given by

$$f(x) \;=\; \frac{c\,\alpha \left[\alpha\, \log(x/\theta)\right]^{c-1} \mathrm{e}^{-\left[\alpha\, \log(x/\theta)\right]^{c}}}{x\,(1-\mathrm{e}^{-1})} \exp\left(\mathrm{e}^{-\left[\alpha\, \log(x/\theta)\right]^{c}} - 1\right). \tag{17}$$

Here and from now on, a random variable X having pdf given by Equation (17) is called the PWP distribution, and is denoted by $X \sim \mathrm{PWP}(c, \alpha, \theta)$. The sf and hrf of X are, respectively, given by

$$S(x) = \frac{\exp\left(\mathrm{e}^{-\left[\alpha\, \log(x/\theta)\right]^{c}} - 1\right) - \mathrm{e}^{-1}}{1 - \mathrm{e}^{-1}},$$

and

$$h(x) = \frac{c\,\alpha\left[\alpha\,\log(x/\theta)\right]^{c-1}\mathrm{e}^{-\left[\alpha\,\log(x/\theta)\right]^{c}}}{x\left\{1-\exp\left(-\mathrm{e}^{-\left[\alpha\,\log(x/\theta)\right]^{c}}\right)\right\}}.$$

Figures 1 and 2 display some plots of the density and hrf of X when $\theta = 1$ for different values of c and α. The plots in Figure 1 reveal that the PWP density can produce various shapes such as reversed-J, approximately symmetric, right-skewed and left-skewed. The plots in Figure 2 indicate that the hrf of X has IFR (increasing failure rate), DFR (decreasing failure rate) and UBT (upside-down-bathtub) shapes.

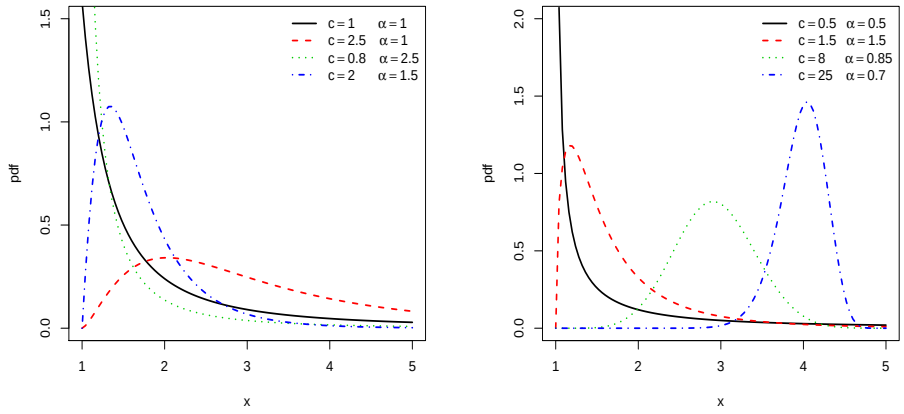

(a) (b)

Figure 1: Plots of the PWP density for some values of c and α with $\theta = 1$.

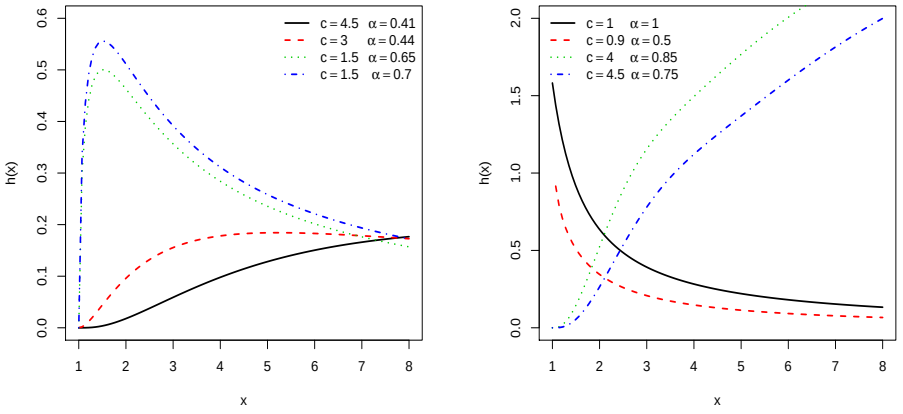

(a) (b)

Figure 2: Plots of the PWP hrf for some values of c and α with $\theta = 1$.

The following lemma gives a relation between the PWP and compound Poisson distributions.

Lemma 5.1. *If a random variable T follows the compound Poisson uniform distribution, then $X = \theta \exp\{\frac{1}{\alpha}\big(- \log(1-T)\big)^{1/c}\} \sim PWP(c, \alpha, \theta)$.*

The following lemma gives the qf of the PWP distribution.

Lemma 5.2. *The qf of X is given by (for $0 < u < 1$)*

$$Q(u) = \theta \exp\Big(\frac{1}{\alpha}\Big[- \log\Big\{1 + \log\big(1 - (1 - \mathrm{e}^{-1})\, u\big)\Big\}\Big]^{1/c}\Big).$$

The following theorem shows the unimodality of the PWP distribution.

Theorem 5.3. *The PWP distribution is unimodal. If $c \leq \theta$, the mode is at $x = \theta$. If $c > 1$, then the mode is at $x = x_0\,\theta$, where x_0 is the solution of the equation $k(x) = 0$, where*

$$k(x) = c\,(\alpha \log x)^c \left[\mathrm{e}^{-(\alpha \log x)^c} + 1\right] + \log x + 1 - c, \quad x > 1. \tag{18}$$

Proof. If $c \leq \theta$, it is easily seen from Equation (17) that $f'(x) < 0$ for all $x > \theta$. Then, $f(x)$ has a unique mode at $x = \theta$. Next, consider $c > 1$. Since $\lim_{x\to\theta} f(x) = 0$, $x = \theta$ cannot be a modal point and therefore $f'(x) = 0$ is equivalent to $k'(x/\theta) = 0$. This implies that the mode of $f(x)$ is at $x = x_0\,\theta$, where $k(x_0) = 0$. Further, the derivative of $k(x)$ is given by

$$k'(x) = \frac{1}{x} + c^2(\alpha \log x)^{c-1}\mathrm{e}^{-(\alpha \log x)^c}\left[1 + \mathrm{e}^{(\alpha \log x)^c} - (\alpha \log x)^c\right].$$

Note that since $\mathrm{e}^{(\alpha \log x)^c} > (\alpha \log x)^c$ for all $x > 1$, this implies that $k'(x) > 0$ for all $x > 1$. So, $k(x) = 0$ has at most one solution. By using the facts that $\lim_{x\to 1} k(x) = 1 - c < 0$ and $\lim_{x\to\infty} f(x) = \infty$, we conclude that $k(x) = 0$ has a unique solution at $x = x_0$ and hence $f(x)$ has a unique mode at $x = x_0\,\theta$. □

5.1. Moments

The following theorem provides some conditions for the existence of moments of the PWP distribution. Let $X \sim \mathrm{PWP}(c, \alpha, \theta)$ and $n \in \mathbb{N}$.

Theorem 5.4. *(i) If $c > 1$, then $E(X^n)$ exists.*
(ii) If $c = 1$, then $E(X^n)$ exists if and only if $\alpha > n$.
(iii) If $c < 1$, then $E(X^n)$ does not exist.

Proof. Without loss of generality, we take $\theta = 1$. Now, letting $u = \alpha \log x$, the existence of $E(X^n)$ is equivalent to the existence of the integral $I = \int_0^\infty u^{c-1}\,\mathrm{e}^{-(u^c - nu)}du$. For $c < 1$, it is clear that $\lim_{u\to\infty} u^{c-1}\,\mathrm{e}^{-(u^c-nu)} = \infty$ and therefore the integral I does not exist. Now, let $c > 1$ and $\phi(u) = u^c - nu$. If $\phi'(m_0) = 0$, then $m_0 = (n/c)^{\frac{1}{c-1}}$ and then $\phi(u)$ is convex and strictly increasing in (m_0, ∞). This implies that there exist constants a and $b > 0$ such that $\phi(u) \geq a + bu$ in (m_0, ∞). Next, we can write $I = \int_0^{m_0} u^{c-1}\,\mathrm{e}^{-\phi(u)}du + \int_{m_0}^\infty u^{c-1}\,\mathrm{e}^{-\phi(u)}du$. Since the first integral on the right hand side is bounded, it is enough to prove the existence of the second one. We have $\int_{m_0}^\infty u^{c-1}\,\mathrm{e}^{-\phi(u)} \leq \int_{m_0}^\infty u^{c-1}\mathrm{e}^{-(a+bu)}du < \infty$ for all $c > 1$ and $b > 0$.
Finally, we consider the last case when $c = 1$. Then, $E(X^n)$ exists iff $J = \int_1^\infty x^{-(\alpha-n+1)}\,\mathrm{e}^{\frac{1}{x^\alpha}}dx$. By using the following inequality

$$\mathrm{e}^x < (1-x)^{-1},\ x < 1 \quad \text{[Abramowitz and Stegun (1972), p. 70]},$$

we have $J < \int_1^\infty \frac{x^{n-1}}{x^\alpha - 1}dx \sim \int_1^\infty x^{-(\alpha-n+1)}dx < \infty$ iff $\alpha > n$. □

Now we derive explicit expressions for the moments of the PWP distribution. Let Z_a follow the exponentiated-Pareto (EP) distribution with shape parameters α and a and scale parameter θ. The cdf and pdf of Z_a are given by

$$F_{EP}(z) = \left[1 - (x/\theta)^{-\alpha}\right]^a \text{ and}$$

$$f_{EP}(z) = \frac{a\,\alpha}{\theta}\,(x/\theta)^{-\alpha-1}\left[1 - (x/\theta)^{-\alpha}\right]^{a-1}.$$

The sth ordinary moment of Z_a (for $s < \theta$) is given by

$$\mathbb{E}(Z_a^s) = \frac{a}{\theta}\sum_{q=0}^{\infty}\frac{(-1)^q}{(q+1)}\,\frac{[\alpha(q+1)\,\theta^s]}{[\alpha(q+1)-s]}\binom{a-1}{q}. \tag{19}$$

The sth incomplete moment of Z_a is given by

$$m'_s(z_a) = \frac{a}{\theta}\sum_{q=0}^{\infty}\frac{(-1)^q}{(q+1)}\,\frac{[\alpha(q+1)\,\theta^s]}{[\alpha(q+1)-s]}\binom{a-1}{q}\left[1 - (z/\theta)^{s-\alpha}\right]. \tag{20}$$

The PWP pdf can be expressed from Equation (11) as a linear mixture of EP pdfs and some of its mathematical properties can be immediately obtained from those of the EP model. The sth ordinary and incomplete moments of X follow easily from Equations (13) & (19) and (14) & (20), respectively.

6. Estimation

The maximum likelihood estimators (MLEs) enjoy desirable properties and can be used when constructing confidence intervals and also in test statistics. The normal approximation for these estimators in large sample distribution theory is easily handled either analytically or numerically. Here we employ the maximum likelihood method.

Let $x_1, \ldots, x_n$ be the observed values from $X \sim \text{PWP}(c, \alpha, \theta)$ and let $\boldsymbol{\rho} = (c, \alpha, \theta)^\top$ be the vector of model parameters. The log-likelihood function for $\boldsymbol{\rho}$ is given by

$$\begin{aligned}\ell &= n\log(c\,\alpha) - n\log\left(1 - \mathrm{e}^{-1}\right) - \sum_{i=1}^{n}\log(x_i) + (c-1)\sum_{i=1}^{n}\log\left[\alpha\log\left(x_i/\theta\right)\right] \\ &\quad - \sum_{i=1}^{n}\left[\alpha\log\left(x_i/\theta\right)\right]^c - \sum_{i=1}^{n}\left[1 - \mathrm{e}^{\left(\alpha\log(x_i/\theta)\right)^c}\right].\end{aligned} \tag{21}$$

The MLE of θ is the first order-statistic $x_{(1)}$ since $x \geq \theta$. Two components of the score vector $U(\boldsymbol{\rho})$ are given by

$$\begin{aligned}U_c &= \frac{n}{c} - \sum_{i=1}^{n}\log\left[\alpha\log\left(x_i/\theta\right)\right] \\ &\quad - \sum_{i=1}^{n}\left[\alpha\log\left(x_i/\theta\right)\right]^c\,\log\left[\alpha\log\left(x_i/\theta\right)\right]\left[1 - \mathrm{e}^{\left(\alpha\log(x_i/\theta)\right)^c}\right], \\ U_\alpha &= \frac{n}{\alpha} + \sum_{i=1}^{n} c\log\left(x_i/\theta\right)\left[\alpha\log(x_i/\theta)\right]^{c-1} \\ &\quad - \sum_{i=1}^{n} c\,\mathrm{e}^{\left(\alpha\log(x_i/\theta)\right)^c}\,\log\left(x_i/\theta\right)\left[\alpha\log(x_i/\theta)\right]^{c-1}.\end{aligned}$$

Setting U_c and U_α equal to zero and solving the equations simultaneously yields the MLEs $(\widehat{c}, \widehat{\alpha})$. The log-likelihood function given in Equation (21) can be maximized either directly by using the OPTIM in the R-language developed by the R Development Core Team (2009), SAS (PROC NLMIXED), Ox program (sub-routine MaxBFGS) or by solving the nonlinear likelihood equations obtained by differentiating (21). These functions were applied and executed for a wide range of initial values. This process often leads to more than one maximum. However, in these cases, we considered the MLEs corresponding to the largest value of the maximized log-likelihood. In a few cases, no maximum was identified for the selected initial values. In these cases, new initial values were tried in order to obtain a maximum point.

6.1. Monte Carlo simulation study

We assess the performance of the maximum likelihood method for estimating the PWP parameters by using Monte Carlo simulation. We consider sixteen parameter combinations, repeat the process 1,000 times under three different sample sizes n=50, 100 and 300. The biases and mean squared errors (MSEs) of the parameter estimates are listed in Table 1. In the simulation study, we consider θ to be unknown and estimate it by the minimum order statistic $x_{(1)}$. The figures in Table 1 indicate that the MLEs are close to the true parameter values, which means that the maximum likelihood method can be used effectively for estimating the parameters of the PWP distribution. The biases decrease as the n increases, as expected.

Table 1: Biases and MSEs for various parameter values.

Sample size	Actual values			Biases			MSEs		
n	c	α	θ	$\tilde{c}$	$\tilde{\alpha}$	$\tilde{\theta}$	$\tilde{c}$	$\tilde{\alpha}$	$\tilde{\theta}$
50	0.5	0.5	1.0	0.0115	0.0501	0.0005	0.0033	0.0373	0.0000
	0.5	0.8	2.0	0.0173	0.0646	0.0009	0.0039	0.0809	0.0000
	0.5	1.0	1.0	0.0155	0.0767	0.0003	0.0036	0.1286	0.0000
	0.5	5.0	2.0	0.0166	0.4598	0.0001	0.0036	3.4630	0.0000
	0.8	0.5	1.0	0.0195	0.0213	0.0095	0.0089	0.0115	0.0002
	0.8	0.8	2.0	0.0266	0.0321	0.0120	0.0099	0.0281	0.0004
	0.8	1.0	1.0	0.0182	0.0479	0.0048	0.0085	0.0463	0.0001
	0.8	5.0	2.0	0.0245	0.2032	0.0019	0.0084	1.1774	0.0000
	1.0	0.5	1.0	0.0310	0.0109	0.0262	0.0148	0.0068	0.0015
	1.0	0.8	2.0	0.0362	0.0251	0.0331	0.0157	0.0173	0.0023
	1.0	1.0	1.0	0.0337	0.0209	0.0127	0.0150	0.0285	0.0003
	1.0	5.0	2.0	0.0235	0.1754	0.0046	0.0129	0.6829	0.0000
	5.0	0.5	1.0	0.1446	0.0022	1.1894	0.3477	0.0003	1.5564
	5.0	0.8	2.0	0.0911	0.0022	1.0395	0.1594	0.0004	1.1618
	5.0	1.0	1.0	0.1658	0.0034	0.4743	0.3424	0.0011	0.2413
	5.0	5.0	2.0	0.1951	0.0149	0.1598	0.3766	0.0256	0.0269
100	0.5	0.5	1.0	0.0081	0.0271	0.0002	0.0016	0.0162	0.0000
	0.5	0.8	2.0	0.0070	0.0381	0.0002	0.0015	0.0374	0.0000
	0.5	1.0	1.0	0.0089	0.0481	0.0001	0.0016	0.0634	0.0000
	0.5	5.0	2.0	0.0034	0.1862	0.0000	0.0016	1.3549	0.0000
	0.8	0.5	1.0	0.0116	0.0111	0.0038	0.0043	0.0055	0.0000
	0.8	0.8	2.0	0.0081	0.0112	0.0050	0.0040	0.0132	0.0001
	0.8	1.0	1.0	0.0112	0.0125	0.0020	0.0038	0.01860	0.0000
	0.8	5.0	2.0	0.0088	0.0900	0.0008	0.0041	0.5225	0.0000
	1.0	0.5	1.0	0.0182	0.0030	0.0126	0.0069	0.0031	0.0003
	1.0	0.8	2.0	0.0087	0.0118	0.0154	0.0062	0.0085	0.0005
	1.0	1.0	1.0	0.0114	0.0100	0.0066	0.0064	0.0121	0.0001
	1.0	5.0	2.0	0.0148	0.0528	0.0025	0.0065	0.3024	0.0000
	5.0	0.5	1.0	0.0561	0.0011	0.9776	0.1568	0.0001	1.0405
	5.0	0.8	2.0	0.0911	0.0022	1.0395	0.1594	0.0004	1.1618
	5.0	1.0	1.0	0.0594	0.0003	0.3970	0.1660	0.0005	0.1692
	5.0	5.0	2.0	0.0930	0.0116	0.1392	0.1772	0.0142	0.0205

Table 1: Continued

Sample size	Actual values			Biases			MSEs		
n	c	α	θ	$\tilde{c}$	$\tilde{\alpha}$	$\tilde{\theta}$	$\tilde{c}$	$\tilde{\alpha}$	$\tilde{\theta}$
300	0.5	0.5	1.0	0.0048	0.0097	0.0000	0.0008	0.0068	0.0000
	0.5	0.8	2.0	0.0029	0.0155	0.0001	0.0007	0.0182	0.0000
	0.5	1.0	1.0	0.0036	0.0183	0.0000	0.0008	0.0267	0.0000
	0.5	5.0	2.0	0.0035	0.0961	0.0000	0.0007	0.6941	0.0000
	0.8	0.5	1.0	0.0060	0.0035	0.0018	0.0019	0.0024	0.0000
	0.8	0.8	2.0	0.0031	0.0097	0.0022	0.0019	0.0065	0.0000
	0.8	1.0	1.0	0.0055	0.0057	0.0008	0.0018	0.0100	0.0000
	0.8	5.0	2.0	0.0071	0.0413	0.0003	0.0019	0.2373	0.0000
	1.0	0.5	1.0	0.0082	0.0025	0.0062	0.0029	0.0015	0.0001
	1.0	0.8	2.0	0.0043	0.0072	0.0077	0.0029	0.0041	0.0001
	1.0	1.0	1.0	0.0128	0.0106	0.0034	0.0030	0.0068	0.0000
	1.0	5.0	2.0	0.0082	0.0202	0.0013	0.0031	0.1632	0.0000
	5.0	0.5	1.0	0.0515	0.0001	0.8026	0.0765	0.0001	0.7036
	5.0	0.8	2.0	0.0263	0.0017	0.8798	0.0748	0.0002	0.8271
	5.0	1.0	1.0	0.0367	0.0005	0.3466	0.0806	0.0002	0.1276
	5.0	5.0	2.0	0.0382	0.0052	0.1191	0.0751	0.0064	0.0150

7. Applications

In this section, we provide three applications of the PWP model. We compare the goodness-of-fit of the PWP model with the fits of the beta Pareto (BP) by Akinsete et al. (2008), Kumaraswamy Pareto (KP) by Bourguignon et al. (2013), exponentiated Pareto (EP) and Pareto (P) Models. For each model, we estimate the parameters by using the method of maximum likelihood and the goodness-of-fit statistics for the models are compared by using the Akaike information criterion (AIC) and Kolmogorov-Smirnov (K-S) statistic. The density functions of the BP and KP models are, respectively, given by

$$\text{BP}: f_{BP}(x;a,b,\alpha,\theta) = \tfrac{1}{B(a,b)}\left(\tfrac{\alpha}{\theta}\right)\left(\tfrac{x}{\theta}\right)^{-\alpha\, b-1}\left[1-\left(\tfrac{x}{\theta}\right)^{-\alpha}\right]^{b-1}, \quad a,b,\alpha>0,\, x>\theta;$$

$$\text{KP}: f_{KP}(x;a,b,\alpha,\theta) = \tfrac{a\, b\, \alpha\, \theta^{\alpha}}{x^{\alpha+1}}\left\{1-\left(\tfrac{x}{\theta}\right)^{-\alpha}\right\}^{a-1}\left[1-\left\{1-\left(\tfrac{x}{\theta}\right)^{-\alpha}\right\}^{a}\right]^{b-1}, \quad a,b,\alpha>0,\, x>\theta.$$

Before progressing further, we provide the histograms of the data sets in Figures 3(b), 4(b) and 5(b). We note that the data sets are reversed-J, right-skewed and approximately symmetric. We further provide the scaled TTT transform (see Aarset (1987)), of the data sets in Figures 3(a), 4(a) and 5(a). The TTT plot for the first data set indicates an increasing failure rate, the one for the second data set reveals an upside-down bathtub and that one for the third data set shows an increasing failure rate.

7.1. Flood Discharge Data

The first real life data set consists of maximum annual flood discharges of the North Saskachevan River and is given in the R-contributed package DAAG. A summary of the data is: n$=48$, $\bar{x}=51.49519$, s$=$ 32.37683, skewness$=2.06859$ and kurtosis$=4.95065$. The MLEs (with SEs in parentheses), AIC and K-S statistics, and K-S p-values are listed in Table 2. Based on these figures, we note that the PWP model gives the best fit. The summary statistics and Figure 3(b) reveal that the first data set is right-skewed. This indicates that the new distribution has the ability to fit data set with right-skewed shape. The P-P plot given in Figure 6 also supports the results of Table 2.

7.2. Plasma Concentration Data

The second real life data set consisting of plasma concentrations of indomethicin is given by Weisberg (2014) and studied by Cordeiro et al. (2014) and Alizadeh et al. (2015). A summary of the data is: n$=66$,

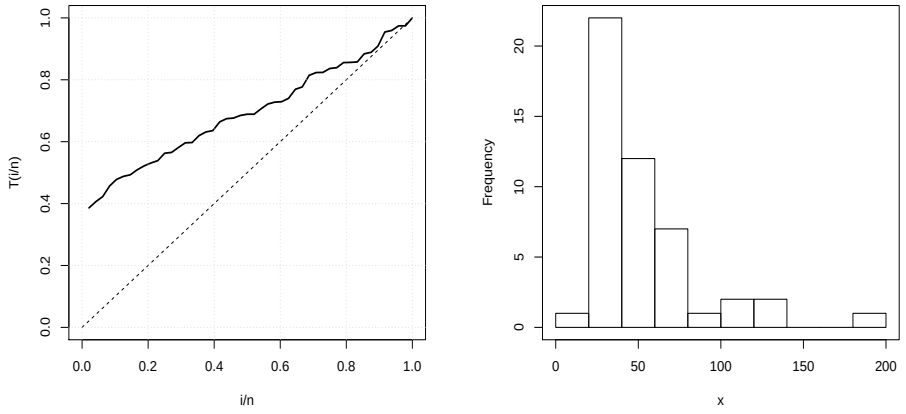

(a) (b)

Figure 3: (a) TTT plot and (b) Histogram of flood discharge data.

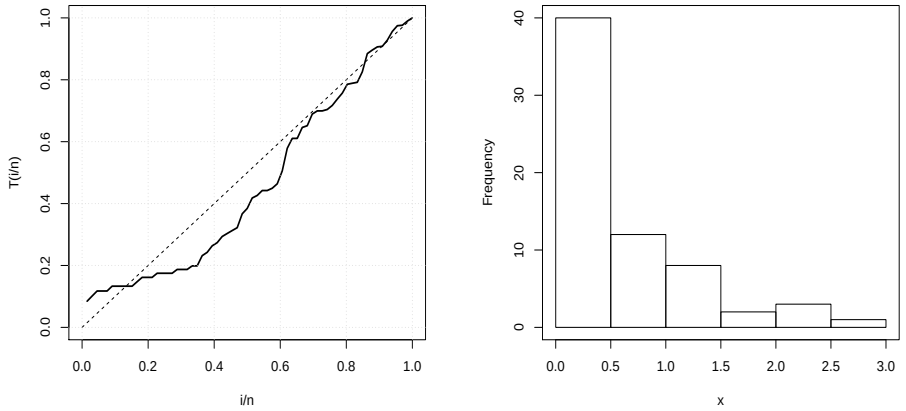

(a) (b)

Figure 4: (a) TTT plot and (b) Histogram of plasma concentration data.

$\bar{x} = 0.59182$, s= 0.632582, skewness= 1.44762 and kurtosis= 1.47087. The MLEs (with SEs in parenthesis), AIC and K-S statistics, and K-S p-value are given in Table 3. From the figures in Table 3, we conclude that the PWP model provides the best fit. A close look at the summary statistics and Figure 4(b) reveals that the second data set is reversed-J shape. This indicates that the new distribution has the ability to fit data with reversed J-shape. The P-P plots given in Figure 7 also support the results of Table 3.

7.3. Carbon Fibre Data

The third data set refers to the failure stresses of single carbon fibres (length 1mm) (Crowder et al. (1991)). A summary of the data is: n= 57, $\bar{x} = 4.2350$, s= 0.8352, skewness= 0.0710 and kurtosis= 2.7098. The figures in Table 4 indicate that the PWP model provides the best fit with the lowest AIC and K-S values.

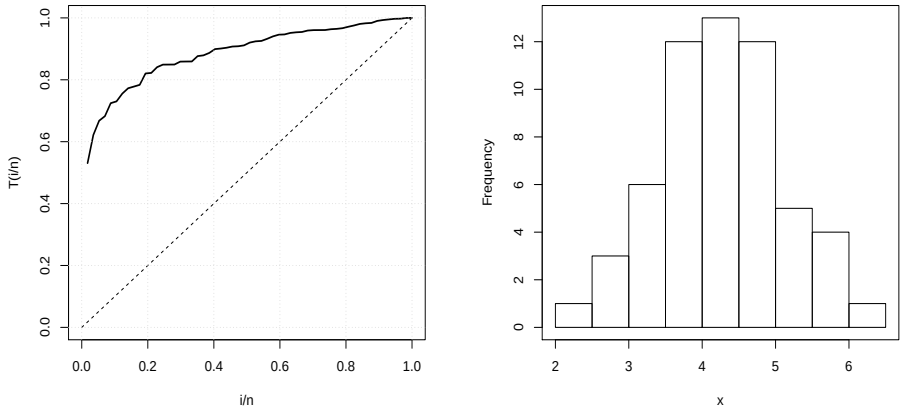

(a) (b)

Figure 5: (a) TTT plot and (b) Histogram of carbon fibre data.

Table 2: MLEs, their standard errors (in parentheses) and goodness-of-fit measures for flood discharge data

Distribution	Estimates				AIC	K-S	p-value
PWP(α, c, θ)	0.9164 (0.2086)	1.8483 (0.0811)	19.885 -		422.4191	0.063	0.9915
BP(a, b, α, θ)	2.3210 (0.4587)	4.8647 (16.9975)	0.5148 (1.6348)	19.885 -	425.5542	0.069	0.5781
KP(a, b, α, θ)	1.7978 (0.2917)	22.9391 (55.3589)	0.2077 (0.3417)	19.885 -	424.4109	0.0604	0.5955
EP(α, a, θ)	1.9971 (0.3048)	2.4403 (0.5426)	19.885 -		424.2743	0.0764	0.3463
P(α, θ)	1.2111 0.1766	19.885 -			436.6653	0.1843	0.0818

Table 3: MLEs, their standard errors (in parentheses) and goodness-of-fit measures for plasma concentration data.

Distribution	Estimates				AIC	K-S	p-value
PWP(α, c, θ)	0.3987 (0.1862)	1.8462 (0.0306)	0.05 -		55.5110	0.1050	0.3865
BP(a, b, α, θ)	2.2383 (0.3693)	6.9608 (17.7514)	0.1556 (0.3697)	0.05 -	59.1441	0.138	0.1889
KP(a, b, α, θ)	1.7970 (0.2172)	25.2028 (26.3843)	0.0845 (0.0598)	0.05 -	58.8954	0.1273	0.2421
EP(α, a, θ)	0.8404 (0.1100)	2.3118 (0.4311)	0.05 -		58.4432	0.1339	0.1942
P(α, θ)	0.5241 (0.0650)	0.05 -			74.5504	0.1568	0.0817

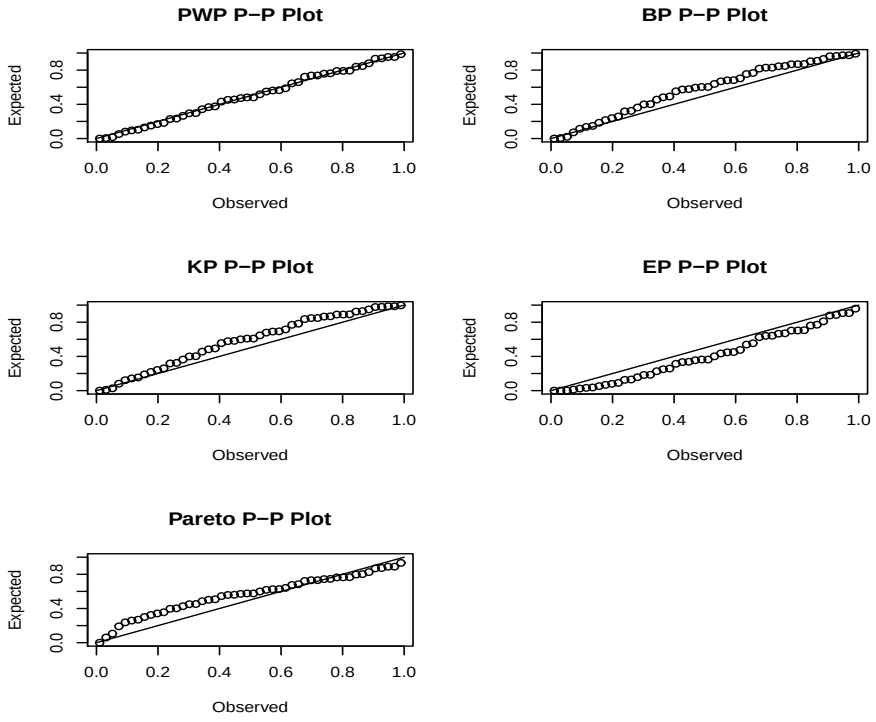

Figure 6: P-P plots of the PWP, BP, KP, EP and P models for flood discharge data.

The summary statistics and Figure 5(b) indicate that the third data set is approximately symmetric. This shows that the PWP model has the ability to fit data with approximately symmetric shape. The P-P plot in Figure 8 also support the results in Table 4.

8. Concluding remarks

We propose a new family of distributions by compounding the Poisson distribution and a sub-class of the T-X family (Alzaatreh et al. (2013)) of distributions called the *Poisson Weibull-X family*. The mathematical properties of the new family such as ordinary and incomplete moments, quantile and generating functions are obtained. Further, a special model of the Poisson Weibull-X family, named the *Poisson Weibull-Pareto (PWP)* distribution, is considered and some of its structural properties are investigated including transformation, modes, ordinary and incomplete moments, quantile and generating functions and mean deviations. The maximum likelihood method is used for estimating the model parameters. The suitability of the maximum likelihood estimates is investigated by a simulation study. We fit the proposed distribution to three real data sets to prove empirically its flexibility.

Acknowledgement.

Authors would like to thank editor-in-chief and an anonymous referee for his constructive comments that improved the earlier version of this manuscript.

References

[1] Aarset, M. V. (1987). How to identify bathtub hazard rate. *IEEE Trans Reliab.*, **36**, 106–108.

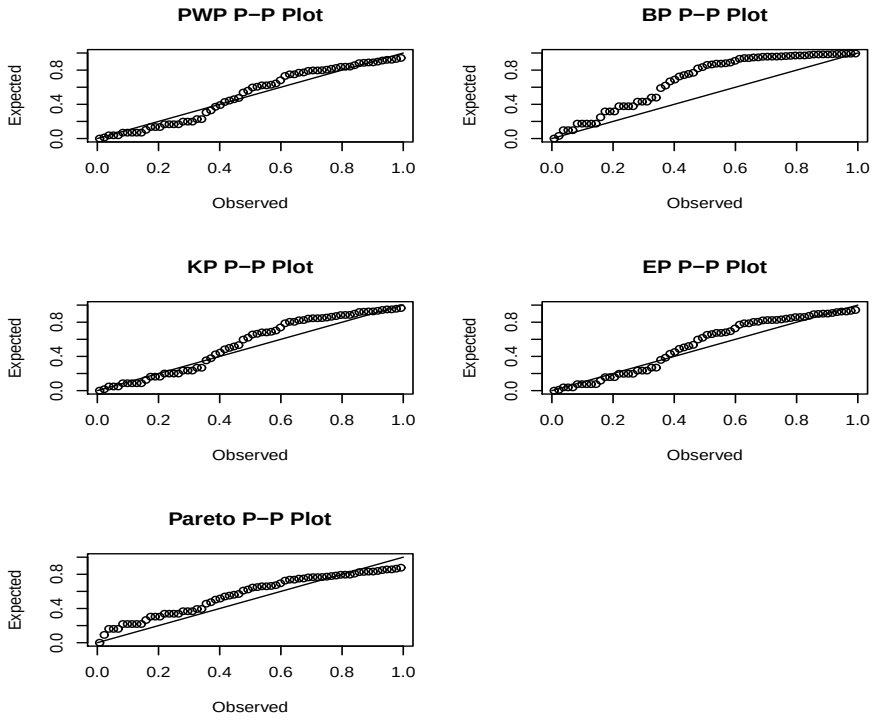

Figure 7: P-P plots for the PWP, BP, KP, EP and P models for plasma concentration data.

[2] Abramowitz, M., and Stegun I. A. (1972). *Handbook of Mathematical Functions with Formulas, Graphs and Mathematical Tables*. Dover Publication, New York.

[3] Akinsete, A., Famoye, F., and Lee, C. (2008). The beta-Pareto distribution. *Statistics*, **42**, 547–563.

[4] Alizadeh, M., Cordeiro, G. M., de-Brito, E., and Demétrio C. G. B. (2015). The beta Marshall-Olkin family of distributions. *J Stat Dist Appl.*, **2**, Art. 4.

[5] Alzaatreh, A., Lee, C., and Famoye, F. (2013). A new method for generating families of continuous distributions. *Metron*, **71**, 63–79.

[6] Bourguignon, M., Silva, M. B., Zea, L. M., and Cordeiro, G. M. (2013). The Kumaraswamy Pareto distribution. *J Stat Theory App.*, **12**, 129–144.

[7] Cordeiro, G. M., Alizadeh, M., and Ortega, E. M. M. (2014). The exponentiated half-logistic family of distributions: Properties and applications. *J Probab Statist.*, Art.ID 864396, 21 p.

[8] Cordeiro, G. M., Ortega, E. M. M., and Nadarajah, S. (2010). The Kumaraswamy Weibull distribution with application to failure data. *J Franklin Inst.*, **347**, 1399–1429.

[9] Crowder, M. J., Kimber, A. C., Smith, R. L, Sweeting, T. J. (1991). *The Statistical Analysis of Reliability Data*. Chapman and Hall. London.

[10] Famoye, F., Lee, C., and Olumolade, O. (2005). The beta-Weibull distribution. *J Stat Theory Appl.*, **4**, 121–136.

[11] Hanagal, D. D., and Dabade, A. D. (2013). A comparative study of shared frailty models for kidney infection data with generalized exponential baseline distribution. *J Data Sci.*, **11**, 109–142.

[12] Kao, J. H. (1956). A new life-quality measure for electron tubes. *IRE Trans Reliab Qual Control*, **7**:1–11.

[13] Lee, E. T., and Wang, J. W. (2003). *Statistical Methods for Survival Data Analysis*. Jhon Wiley & Sons, New York.

[14] McGilchrist, C. A., and Aisbett, C. W. (1991). Regression with frailty in survival analysis. *Biometrics.*, **47**, 461–466.

[15] Mudholkar, G. S, and Srivastava, D. K. (1993). Exponentiated Weibull family for analyzing bathtub failure data. *IEEE Trans Reliab.* **42**, 299–302.

[16] Nadarajah, S., and Kotz, S. (2006). The exponentiated type distributions. *Acta Appl Math.*, **92**, 97–111.

[17] R Development Core Team. (2009). *A Languge and Environment for Statistical Computing*. Austria, Vienna: R Foundation for Statistical Computing.

[18] Weibull, W. (1951). A Statistical distribution function of wide applicability. *J Appl Mech*, **18**, 293–297.

[19] Weisberg, S. (2014). *Applied Linear Regression*. John Wiley & Sons, New York.

Table 4: MLEs, their standard errors (in parentheses) and goodness-of-fit measures for carbon fibre data.

Distribution	Estimates				AIC	K-S	P-value
PWP(α, c, θ)	1.3411 (0.0490)	4.1029 (0.4302)	2.247 -		136.480	0.057	0.9893
BP(a, b, α, θ)	9.0992 (1.7259)	17.3704 (26.8925)	0.6900 (0.9078)	2.247 -	145.515	0.100	0.5911
KP(a, b, α, θ)	4.9429 (1.1999)	50.0216 (9.9178)	0.8797 (0.6503)	2.242 -	149.3523	0.1273	0.2421
EP(α, a, θ)	4.9620 (0.5288)	12.7885 (3.5442)	2.242 -		150.2419	0.1339	0.1942
P(α, θ)	1.6006 (0.2139)	2.242 -			221.955	0.1568	0.0817

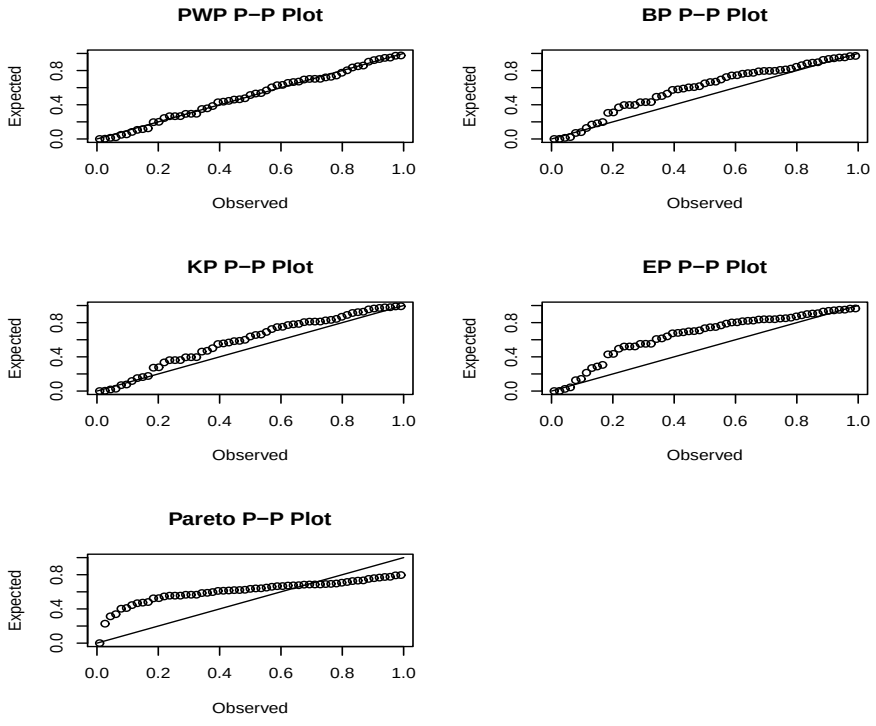

Figure 8: P-P plots for the PWP, BP, KP, EP and P models for carbon fibre data.